Modernized Control Laws for UH-60 BLACK HAWK Optimization and Flight-Test Results

Mark B. Tischler,* Christopher L. Blanken,† Kenny K. Cheung,‡ and Sean S. M. Swei§
Ames Research Center, Moffett Field, California 94035-1000
and
Vineet Sahasrabudhe¶ and Alexander Faynberg**
Sikorsky Aircraft Corporation, Stratford, Connecticut 06601-1381

Modernized control laws were developed to provide an attitude-command/attitude-hold response type for the UH-60 BLACK HAWK helicopter and thereby afford improved handling qualities for near-Earth operation in night and poor weather. The inner-loop system modernized control laws were implemented using the 10% authority stability augmentation system actuators and was evaluated in an EH-60L helicopter. Central to addressing the significant resource and technical challenges of this project was the extensive use of a modern integrated tool set. System identification methods provided an accurate flight-identified aircraft response model and allowed the efficient isolation of discrepancies in the block diagram-based simulation model. Additional key tools were real-time rapid prototyping and a well-designed picture-to-code process. Control laws were tuned to achieve the maximum design margin relative to handling qualities and control system performance requirements. The optimized design was seen to be robust to uncertainties in the identified physical parameters. A flight-test evaluation by three test pilots showed significant benefits of the optimized design compared to the BLACK HAWK standard flight control configuration.

Introduction

SIKORSKY Aircraft Corporation (SAC), under a National Rotorcraft Technology Center project, is developing modernized flight control laws for legacy aircraft that operate in the degraded visual environment. [The term modernized control laws used throughout this paper refers to the updated control laws discussed in this project as compared to UH-60 helicopter legacy control laws and not modern control, for example, H^∞, linear quadratic regulator, (LQR), etc., as is common in the control literature.] The baseline aircraft for this effort is the UH-60 BLACK HAWK helicopter. These control laws are aimed at providing an attitude-command/attitude-hold (ACAH) control response using the existing partial authority flight control augmentation actuation system. An ACAH control response is an essential element in retaining satisfactory handling qualities for near-Earth operations as the pilot's visual cues degrade, such as for night and poor weather operations.[1] The inner-loop system, referred to as modernized control laws-2 (MCLAWS-2) (read as MCLAWS minus-two), is intended to achieve an ACAH response type in near-hovering flight (up to 20–30 kn) by using the stability augmentation system (SAS) servos only. This sys-

tem forms the basis for the final system tested at Ames Research Center (MCLAWS-1), which incorporates parallel trim servos in an outer loop to help recenter the SAS servos and minimize saturation for higher-speed operations up to 50 kn (as discussed in Ref. 2).

The MCLAWS-2 was first assessed in ground-based piloted simulations at both Sikorsky and the Ames Research Center Vertical Motion Simulator. One of the key results from these ground-based simulations[3] was that the ACAH response in pitch and roll improved the handling qualities in the hover/low-speed flight regime. Also, the improvements found were consistent across a range of mission task elements for both the good and degraded visual environment. To extend the simulation results and reduce the risk for implementation onto production aircraft, a flight-test assessment was undertaken and performed in cooperation with SAC on the U.S. Army/NASA EH-60L BLACK HAWK helicopter. (The actual test aircraft was a prototype EH-60L Advance QuickFix aircraft that was modified for flight testing. All external antennas and aircraft survivability equipment were removed from the aircraft, making the airframe response to flight control system inputs the same as a standard EH-60L.) The initial flight assessment reported herein was performed in the daytime with a good visual environment. The objective was to evaluate the MCLAWS-2 on a BLACK HAWK by using the existing SAS partial authority servos. These servos provide ±10% authority relative to the pilot's control. (By convention, cockpit stick throw has a range of 0–100% corresponding to 0-10 in. of travel. Maximum command of the SAS produces ±1-in. equivalent stick motion, which is referred to as a ±10% authority system.) For the flight test, the approach was initially to compare and validate the control law responses between simulation and flight and, if necessary, reoptimize the control law gains to account for observed modeling discrepancies and aircraft implementation issues. Once optimized, the team performed a handling quality evaluation using Aeronautical Design Standard (ADS-33) (Ref. 1).

The design, optimization, and flight testing of the modernized partial authority control laws on the EH-60L constituted both technical and resource challenges. The primary technical challenges were to meet the competing design objectives of ADS-33 and other relevant design requirements, for example, short-term response, stability, disturbance rejection, degree of saturation, using the limited (±10%)

*Senior Technologist, Aeroflightdynamics Directorate, U.S. Army Aviation and Missile Research, Development, and Engineering Center, N243-11; mtischler@mail.arc.nasa.gov. Associate Fellow AIAA.

†Research Scientist, Aeroflightdynamics Directorate, U.S. Army Aviation and Missile Research, Development, and Engineering Center, N243-11; cblanken@mail.arc.nasa.gov.

‡Principal Flight Control Software Engineer, University of California at Santa Cruz; kcheung@mail.arc.nasa.gov. Member AIAA.

§Principal Research Engineer, University of California at Santa Cruz; sswei@mail.arc.nasa.gov. Member AIAA.

¶Principal Engineer, Handling Qualities and Control Laws; vsahasrabudhe@sikorsky.com.

**Senior Engineer, Handling Qualities and Control Laws; afaynberg@sikorsky.com.

available SAS control authority and given the significant hardware system lags. This was accomplished using optimization-based control system design methods based on an accurate mathematical model. The resource challenges of a 3-week project schedule and a total of 6 flight-test hours available for the development and piloted evaluation of the MCLAWS-2 system stands in contrast to typical recent example of about 28 flight test hours over 8 weeks to optimize the stability and control augmentation system gains of the OH-58D(R) (Ref. 4). Central to addressing these technical and resource challenges, and the focus of this paper, was the extensive use of a modern integrated tool set.

The key elements of the integrated tool set were block diagram simulation (SIMULINK®),[5] system identification (CIFER®),[6] control system analysis and optimization (CONDUIT®),[7] real-time rapid prototyping (RIPTIDE),[8] and pictures-to-code conversion. A detailed block diagram model of the partial authority system implementation in the EH-60L was developed in SIMULINK as the basis for control law analysis and optimization. Central to the simulation was an accurate flight dynamics model. One of the most accurate BLACK HAWK models is that of the JUH-60A airframe obtained from frequency-domain system identification studies[9] using the comprehensive identification from frequency responses (CIFER) facility. CIFER was also used extensively to isolate and correct modeling discrepancies based on subsystem and end-to-end frequency-response comparisons of the simulation vs the EH-60L flight data. Control law evaluation and optimization was completed using the control designer's unified interface (CONDUIT), which proved an effective tool to reach rapidly a design solution that met the competing objectives with minimum overdesign. Control laws were implemented using pictures-to-code techniques (MATLAB® Real-Time Workshop Embedded Code Generation[10]) to eliminate hand coding of control system block diagrams and updates. Final control-law checkout, including mode blending, actuator saturation, and piloted evaluation of the MCLAWS-2 control law implementation before flight was conducted using the U.S. Army Aeroflight-dynamics Directorate- (AFDD)-developed desktop simulation referred to as the Real Time Interactive Prototype Technology Integration Development Environment (RIPTIDE). The RIPTIDE simulation incorporated a full nonlinear model of the UH-60A based on GENHEL (Ref. 11) and the actual real-time flight control code (as produced by MATLAB pictures to code) to evaluate important implementation issues such as mode transitions, saturation effects, control system initialization, and limited piloted preflight evaluation.

This paper presents the methodology and results of using the integrated tool set for development, optimization, and flight testing of the MCLAWS-2 for the EH-60L. First, an overview is presented of the MCLAWS-2 concept and hardware implementation on the EH-60L aircraft. The next section presents the analysis methods used for modeling, control system evaluation, and model discrepancy isolation. Example results of the corrected model show excellent agreement with the system identification flight-test data for a baseline gain set. The isolation of modeling discrepancies in the individual hardware blocks and the numerical buildup of broken-loop flight response using system identification techniques was important to the success of the program and is illustrated in detail. A primary focus of the paper is on handling-qualities analyses and control system optimization using CONDUIT. Optimization based on design margin is shown to provide a family of designs based on uniformly increasing performance. This design approach is validated with the flight results. The robustness analysis based on the uncertainty bounds of the identified physical model parameters and the identification model structure is also a unique aspect of this paper. The final section covers the flight evaluation of the optimized MCLAW-2 configurations, showing significant qualitative and quantitative performance benefits compared to the EH-60L standard SAS/flight-path stabilization system (FPS) flight control system.

MCLAWS-2 Concept and Implementation

The principal objective of the modernized control laws is to provide the pilot with an ACAH response type. However, in a partial authority system, this places a challenge on the design of the control laws to operate without saturating the SAS servo authority limit. Whereas transiently touching the limits may be acceptable, especially during maneuvers, prolonged saturation leaves the helicopter with no augmentation whatsoever. Whereas trim servos are useful to help keep the SAS servos centered and reduce saturation in steady flight, their use in the inner loop to achieve ACAH control response can result in undesirable stick motions being seen by the pilot. The challenge addressed here is to achieve the ACAH control response in the existing aircraft using the 10% SAS authority limits and available sensor complement, and computational power.

The basic structure of the MCLAWS-2 investigated in this study is shown in Fig. 1. Figure 1 shows the pitch-axis structure only; the roll and yaw axes have a similar structure. Also shown for comparison is the structure of the current pitch-axis control laws that are part of the SAS on current UH-60A aircraft. The current pitch SAS is essentially a rate feedback system that augments the damping of the bare airframe dynamics. As mentioned, the MCLAWS-2 system implements an ACAH response type using only the 10% SAS series servos (no trim actuators). The CONDUIT-optimized system achieves ACAH with little to no saturation for near hover out to 20–30 kn. The MCLAWS-1 (with trim) has been demonstrated to extend the benefits of ACAH out to 50 kn (Ref. 2) without significant saturation.

The MCLAWS-2 implements a two-mode control system. In the attitude mode the pitch and roll axes have ACAH-type responses, whereas the yaw axis has rate-command/direction-hold characteristics. The pitch and roll control laws switch to a rate command mode if the helicopter velocities or attitudes exceed the limits shown in Table 1, though later flight experience indicates handling-qualities advantages to extending this out to higher speeds.[2] As the name indicates, in the rate mode the aircraft has a rate command response type. To switch back to attitude mode from rate mode, more restrictive conditions must be met, which are also shown in Table 1. When the system switches from attitude mode to rate mode, the dashed paths
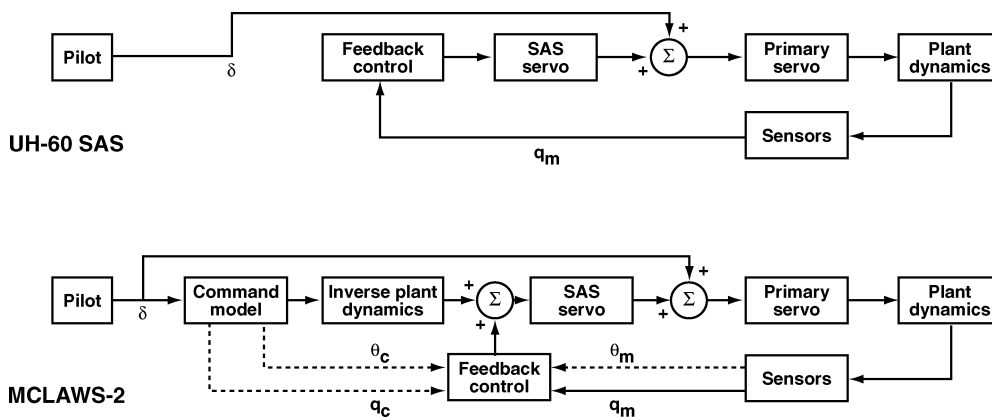

Fig. 1 Standard UH-60 and MCLAWS schematic diagrams.

Table 1 Attitude to rate mode switching thresholds

Aircraft state	ACAH will engage if	ACAH will disengage if
$|\theta|$	<15 deg and	>25 deg or
$|\phi|$	<10 deg and	>35 deg or
$\sqrt{(U^2 + V^2)}$	<20 kn	>30 kn

in Fig. 1 are removed gracefully, and the systems revert back to a rate feedback architecture almost identical to the baseline UH-60A SAS control laws. Conversely, when the aircraft reenters the attitude mode, these paths are brought back in gradually. The overall objective was to retain ACAH characteristics over a useful range of aircraft velocities and attitudes without persistently saturating the SAS.

The initial gain set for the MCLAWS-2 flight-test effort (referred to herein as baseline) was based on linear analysis, extensive nonlinear piloted simulation (as described in Ref. 3), and an initial analysis using CONDUIT. These initial simulation and analysis studies indicated satisfactory performance for a range of stability and handling qualities requirements. The focus of this paper and the flight-test results presented are for the ACAH mode only.

EH-60L Integration

The implementation of the MCLAWS-2 onto the U.S. Army/NASA EH-60L helicopter included the installation of a research flight control computer (RFCC), a switch for selection between the EH-60 standard SAS or the RFCC, and features to ensure satisfactory engagement/disengagement of the RFCC. For example, interlock features were designed into the system to prevent engagement if the RFCC is not functioning properly or if the aircraft air data system is not available. In addition, dummy electrical loads were switched in for the servos to satisfy the EH-60 SAS and flight-path stabilization system (SAS/FPS) monitors so that reversion from the RFCC was to the standard EH-60 SAS with trim on. (No ground mode was implemented herein.) The RFCC was engaged in the air, with all takeoffs and landings performed with the standard EH-60 SAS/FPS.

A key aspect of the integration was the ease with which the modern control laws could be transferred between SAC and the AFDD, analyzed, simulated on the ground before flight, and transferred onto the aircraft. MATLAB/SIMULINK control law block diagrams were central to this process (Fig. 2). The pictures-to-code pathway between analysis, simulation tools, and the aircraft used the MATLAB Real-Time Workshop Embedded Coder for rapid turnaround and very cost-effective design iteration. A final iteration step was the ability to change some control law parameters onboard the aircraft while in flight. The control laws and proposed modifications were evaluated in the RIPTIDE ground-based simulation environment for piloted preflight check out just before implementing them in the aircraft.

SIMULINK Analysis Model

In parallel with the MCLAWS-2 implementation into the EH-60L, a detailed model of the helicopter and control system was developed in SIMULINK (Fig. 3) for analysis and optimization of the ACAH mode in low-speed/hovering flight. This model was initially evaluated using CONDUIT to document expected broken-loop and closed-loop response characteristics for the baseline set of MCLAWS-2 gains. The SIMULINK model for the ACAH control mode comprised 91 states, including key elements of attitude command and feedback loops of the SAS represented by transfer functions; flight-identified 36-state bare-airframe linear model; SAS servoactuators, pitch, roll, and yaw channels; primary servoactuators, pitch, roll, yaw, and collective channels; and transport (Padé) delay approximation of phase-lag contribution by sensor dynamics.

The model of the bare-airframe response to mixer input is a central element of the SIMULINK simulation and determines to a large extent the overall accuracy of the control system analysis. Fletcher and Tischler[9] extracted an accurate (linear) state-space representation of the JUH-60A dynamics for hover/low-speed flight from flight data by using CIFER,

$$M\dot{x} = Fx + Gu, \qquad y = Hx + Ju \qquad (1)$$
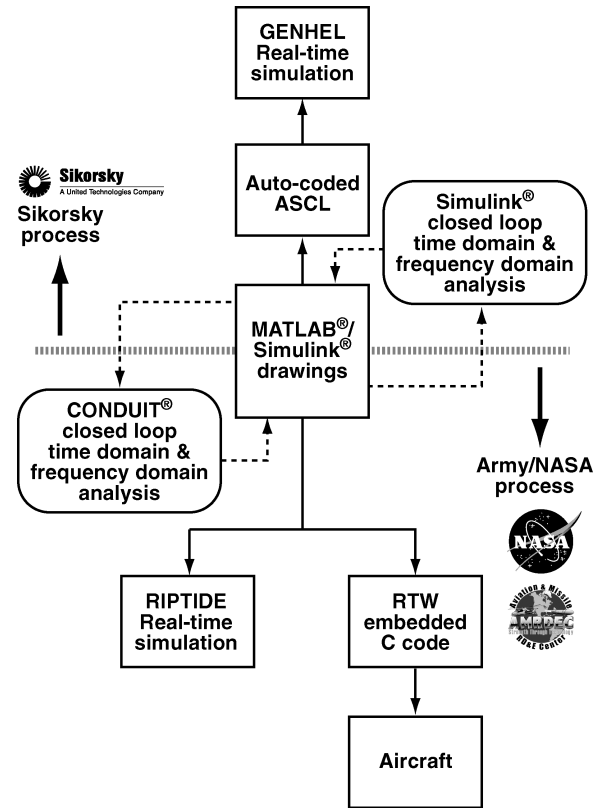
Fig. 2 Pictures-to-code process.

The bare airframe model comprises 36 states and includes the dynamics of the fuselage, rotor flapping, rotor lead–lag, engine/governor/fuel system, dynamic inflow, and aerodynamic phase lag. The model is valid over the frequency range of 0.5–40 rad/s and is well suited for flight control applications.[12] Other applications of this model have included full authority fly-by-wire flight control design,[13] gust response modeling,[14] and envelope limiting and cueing.[15] An important additional product of the system identification study was the set of 1σ confidence bounds for each identified parameter. These confidence bounds were used to evaluate the robustness of the optimized control system to parameter uncertainty, as discussed later. As part of the integrated tool set, the state-space model and 1σ confidence bounds were retrieved directly from the CIFER database for use in the SIMULINK analysis model.

An accurate representation of the actuator dynamics is also of key importance to overall accuracy of the analysis. Previous studies used CIFER to extract an accurate second-order transfer-function model of the actuator dynamic response from flight-test data. The model was implemented in state-space form and included actuator rate and position saturation limits.

Determination of Discrepancies in SIMULINK Analysis Model

Initial flight tests of the baseline gain set showed significant qualitative discrepancies with the predicted characteristics based on the SIMULINK analysis model. An immediate project decision was made to conduct ground and flight tests to establish the source of these discrepancies and achieve a reliable anchor point for further design optimization using CONDUIT. The tests and analysis were completed in a one week focused effort that is illustrated in the following paragraphs.

Frequency sweeps in pitch, roll, and yaw were conducted for the MCLAWS-2 baseline gain set at the hover flight condition in 1 h of flight time. Standard frequency-sweep test techniques were used,[16] with maximum input amplitudes and frequencies kept within a range that avoided limiting of the SAS actuators, that is, less than ±10% stick input. Example flight data for a roll sweep are shown
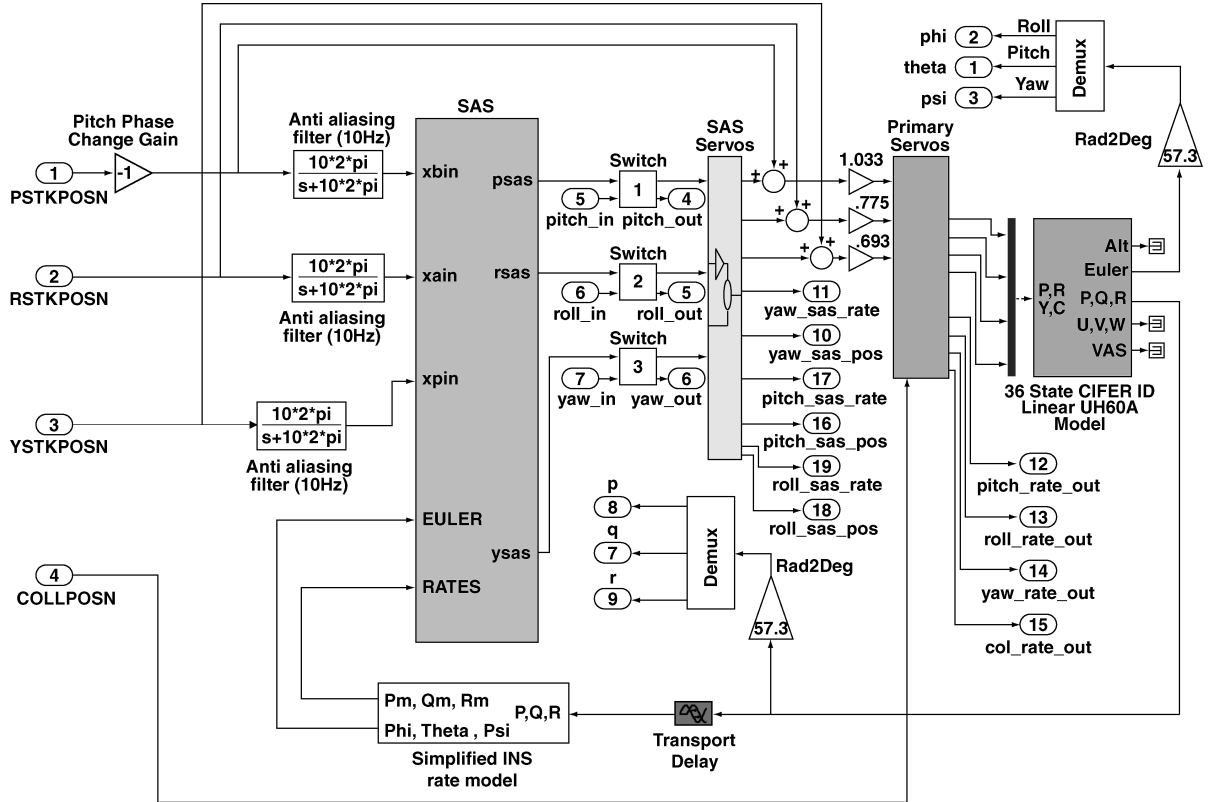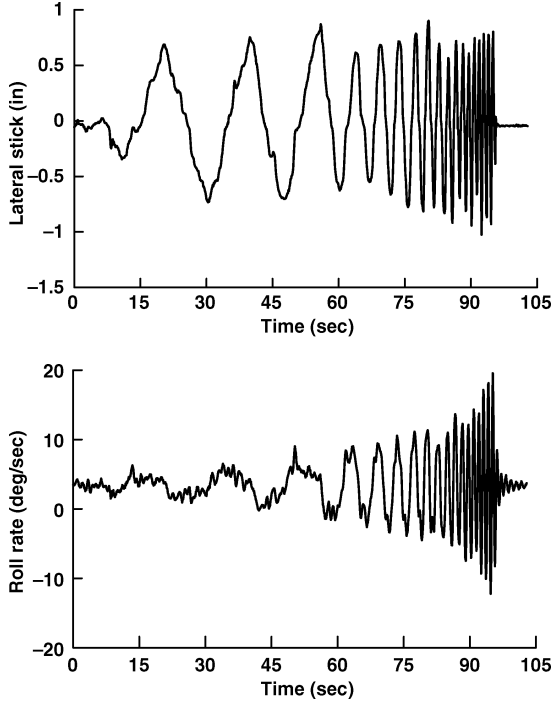
Fig. 3 MCLAWS-2 ACAH SIMULINK block diagram.

Fig. 4 Flight-test data for roll frequency sweep.

FCC signals were recorded in the flight tests, a result of careful preflight planning. This allowed frequency-response identification of the key elements of the block diagram, which proved invaluable for isolating the various modeling discrepancies. Phase errors were observed in elements that should have been easily and accurately modeled, such as the command model and SAS actuator response. Some quick, but insightful, bench tests were conducted on the measurement system that exposed timing skews of up to 44 ms between the various measurement signals as the source of the observed phase errors. These skews were artifacts of the measurement system itself and were not present in the MCLAWS-2 feedback quantities. The effects of these timing skews were corrected in the identification results, thereby allowing a valid comparison of the measured responses with the SIMULINK model and an isolation of the remaining errors.

A second source of discrepancy between the analysis model and the actual flight hardware integration was in the various control throws. The initial MCLAWS-2 control law design for the EH-60L as provided by SAC incorporated control system gains based on the idealized definitions of stick throw, SAS actuator throw, stick-to-mixer gearing, and mixer-rotor head gearing, as embodied in the GENHEL simulation.[11] On the other hand, the CONDUIT/SIMULINK analysis was based on direct measurements and carefully calibrated gearing as determined using CIFER from ground-based measurements taken in the JUH-60A and EH-60L helicopters. The inconsistencies in the various gearings and mixings resulted in fairly sizable magnitude shifts (and, thus, scale factor errors in the proper gain settings) for the EH-60L bare-airframe response as compared to the initial design models. Several additional discrepancies between the SIMULINK modeling and aircraft implementation of the MCLAWS-2 control laws were also found and corrected.

The frequency response of the corrected SIMULINK block elements of Fig. 5 were determined using CONDUIT and were rechecked against the flight data. Excellent agreement in all of the axes was found both for the individual block elements as well as for the overall broken-loop and closed-loop responses. Some examples for the roll axis follow.

in Fig. 4. Three repeat roll sweeps were flown and concatenated in CIFER for improved identification accuracy. The initial comparison of the system identification results with the SIMULINK model verified that some significant mismatches in the gain and phase responses were the likely cause of the observed qualitative discrepancies.

The simplified roll-axis schematic of Fig. 5 illustrates the flight-test measurements available. As can be seen, many of the internal
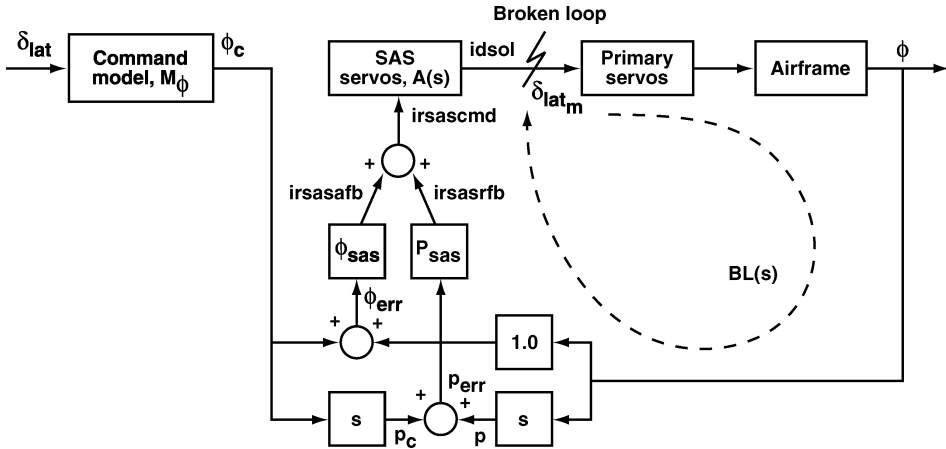
Fig. 5   Simplified schematic of roll axis MCLAWS-2 implementation; measured parameters indicated next to signal arrows.

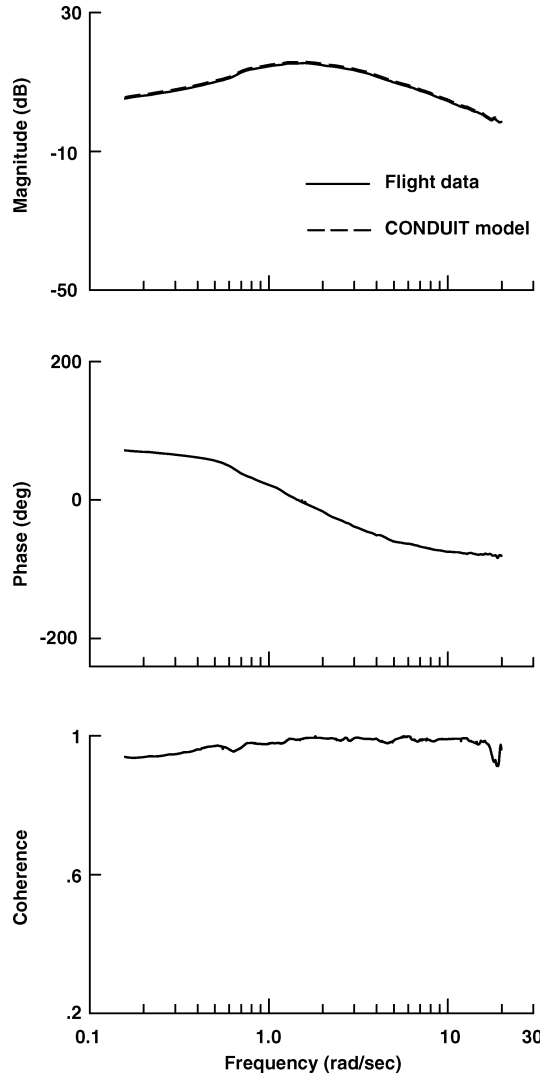Fig. 6   Command model comparison [$sM_\phi(s)$], roll axis.

Fig. 7   Roll rate SAS compensation comparison, P_{sas}.

The roll-rate command-model response, $sM_\phi(s)$ of Fig. 5 in degrees per second per inch, is identified from the recorded time histories,

$$sM_\phi(s) = p_c(s)/\delta_{\text{lat}}(s) \qquad (2)$$

and is compared in Fig. 6 with the ideal command model as represented in the CONDUIT analysis,

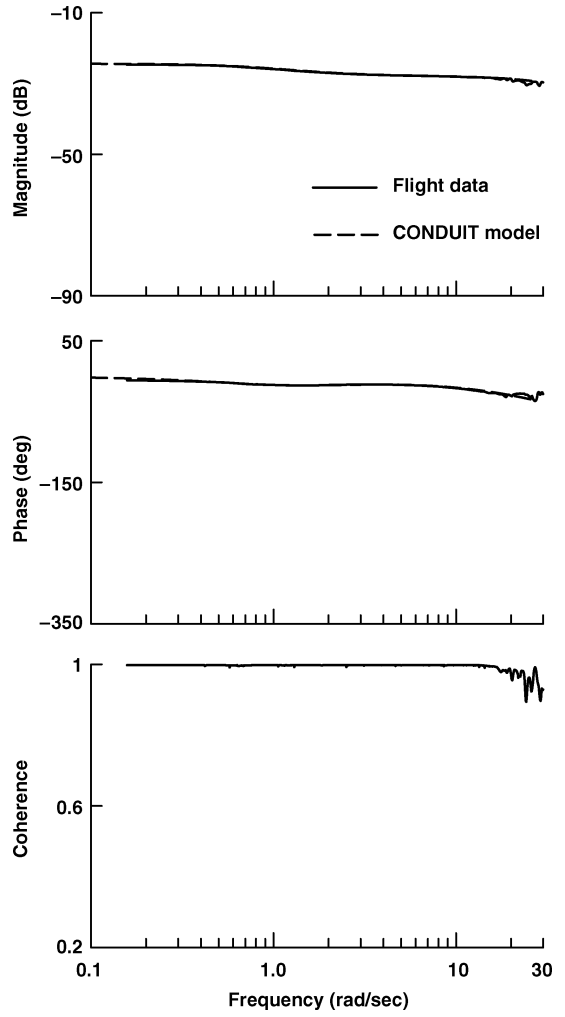$$[sM_\phi]_{\text{CONDUIT}} = \frac{7.16s}{(0.625s + 1)(0.625s + 1)} \qquad (3)$$

The coherence is nearly unity, indicating excellent accuracy as would be expected for identifying software elements as compared to airframe dynamics. The roll rate SAS dynamics, $P_{\text{sas}}(s)$ of Fig. 5, are identified $[P_{\text{sas}}(s) = ir\text{sas}rfb(s)/p_{\text{err}}(s)]$ and again match the CONDUIT model precisely as shown in Fig. 7. The unaugmented response of the helicopter to mixer input is $p(s)/\delta_{\text{lat}_m}(s)$, which includes both the bare airframe and primary servos as seen in Fig. 5. As shown in Fig. 8, the comparison of the EH-60L flight data and CONDUIT analysis model are in good agreement in the frequency range of good coherence (0.5–20 rad/s) once the scale factor

Table 2 Roll broken-loop and closed-loop response metrics for baseline gain set

Analysis	ω_c, rad/s	Phase margin, deg	Gain margin, dB	ω_{180}, rad/s	Bandwidth, rad/s	Phase delay, s
CONDUIT	3.30	64.8	8.27	8.62	2.63	0.0762
Flight	2.74	73.0	9.68	9.05	2.03	0.0766
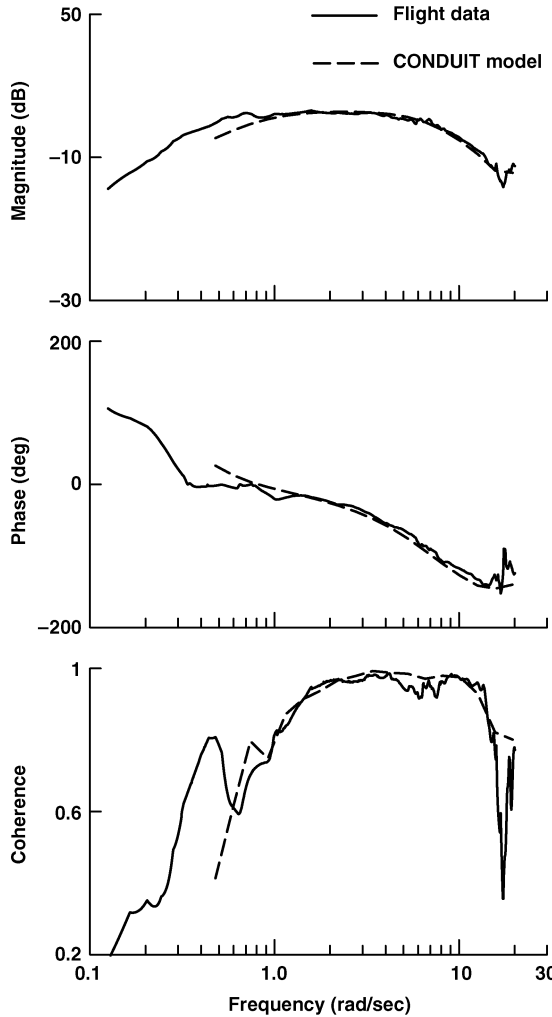
Fig. 8 Unaugmented roll response comparison, p/δ_{lat_m}.

Fig. 9 Roll broken-loop response comparison, Eq. (4).

corrections discussed earlier are included. The broken feedback loop response [indicated as $BL(s)$ in Fig. 5] is critical for determining crossover frequency and stability margins and is obtained by multiplying the individual identified responses using the frequency-response arithmetic function in CIFER,

$$BL(s) = [s\,P_{\text{sas}}(s) + \phi_{\text{sas}}(s)]\big[\big(p(s)\big/\delta_{\text{lat}_m}(s)\big)(1/s)\big][A(s)] \quad (4)$$

making direct use of the frequency-response data, for example, $P_{\text{sas}}(s)$ of Fig. 7 and the unaugmented helicopter response $p(s)/\delta_{\text{lat}_m}(s)$ of Fig. 8. The broken-loop response for roll shows very good agreement with the analysis model as seen in Fig. 9. This ensures that the key control system metrics of crossover frequency, gain margin, and phase margin will be well predicted. Finally, the overall closed-loop response of $p(s)/\delta_{\text{lat}}(s)$ shows good agreement, as can be seen in Fig. 10, thereby ensuring that the handling-qualities parameters (bandwidth and phase delay) will be well predicted.

A summary of the broken-loop and closed-loop response metrics for the roll loop is presented in Table 2 for the baseline MCLAWS-2 gain set. The CONDUI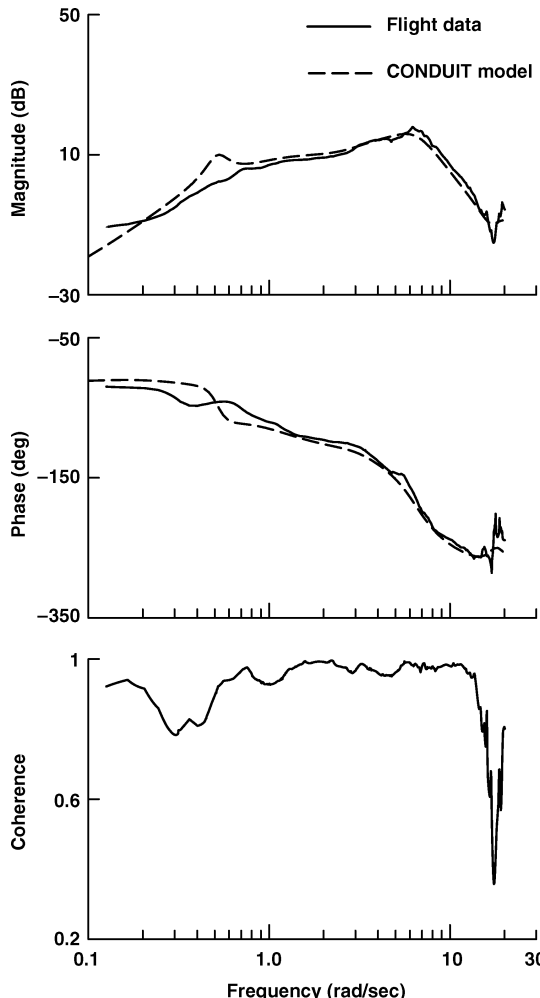T predictions are generally seen to match the flight data quite well, as is expected from the good agreement in the frequency responses shown earlier. Similar levels of agreement were achieved for the pitch and yaw channels. This analysis established that the updated CONDUIT model provided a satisfactory anchor point (MCLAWS-2 baseline) from which design optimization was conducted.

CONDUIT Baseline Analysis

Eight unique types of specification listed in Table 3 were selected for the baseline gain set analysis. Some specifications were chosen to assess response vs ADS-33 handling qualities and MIL-F-9490D stability requirements, whereas others were Ames Research Center derived and selected to address performance issues. The eigenvalues specification verifies that the closed-loop system is stable. The stability margin specification verifies that satisfactory gain and phase margins are achieved for the broken-loop responses. In the yaw axis, the evaluation is completed for both: rate and attitude feedback (feet off pedals) and rate feedback only (feet on pedals). The bandwidth specifications are key short-term response requirements in ADS-33 and are directly related to the step-response rise time. The damping ratio specification determines the damping ratio of all

Requirements	Source	Specification	Channel	Constraint type
Eigenvalues	Ames Research Center	EigLcG1	——	Hard
Stability margins	MIL-F-9490D	StbMgG1	Pitch, roll, and yaw	Hard
Bandwidth	ADS-33	BnwAtH1	Pitch and roll	Soft
Damping ratio	Ames Research Center	EigDpG1	——	Soft
Crossover frequency	Ames Research Center	CrsLnG1	Pitch	Objective
Actuator rms	Ames Research Center	RMSAcG1	Pitch	Objective
Bandwidth	ADS-33	BnwAtH1	Yaw-rate feedback	Check only
Pitch and roll coupling	ADS-33	CouPRH2	Pitch/roll	Check only

As can be seen from Fig. 11, the roll axis for the baseline design predicts overall satisfactory HQ and control system performance, with all specifications meeting the level-1 requirements. The yaw characteristics are also satisfactory, except for yaw bandwidth (BnwAtH1), which achieves only level-3 HQ. Finally, the pitch axis displays a level-3 stability margin (StbMgG1) and level-2 bandwidth (BnwAtH1), the latter resulting from a very low crossover frequency (CrsLnG1). The pitch–roll coupling, seen as borderline level-2/level-3, is unchanged from the standard EH-60L and results both from the inherent coupling of all rotorcraft, as well as the influence of the canted tail rotor. Crossfeeds were developed in analysis and found to be effective in reducing pitch–roll coupling, but were not evaluated during the limited flight program.

Note that the same baseline evaluation discussed in this section was originally conducted on the uncorrected simulation model, before the determination and resolution of model discrepancies. These original results showed better (and thus misleading) performance in general. This finding underlies the importance of having a well-validated aircraft model to minimize flight-test time and achieve improved HQ in a rational and predictable manner.

A preliminary flight-test evaluation was conducted for the MCLAWS-2 baseline gain set, that is, without optimization, to provide some initial pilot comments. The following key comments related to HQ issues: 1) "no residual roll oscillations following lateral pulse," 2) "no cross coupling following the longitudinal pulse," 3) "configuration was stable with the exception of one–two cycles of roll oscillation after achieving a stabilized hover," 4) "very nice attitude command response during the maneuver," 5) "three to four cycles of roll oscillations occurred following the feet-off the micro-switches pedal input," 6) "maneuver performed within desired tolerances, but longitudinal drift resulted in some excursions into adequate," and 7) "longitudinal and lateral drift more pronounced."

These pilot comments generally track the CONDUIT baseline evaluation results of Fig. 11. A consensus was reached that emphasis for design improvement was needed on the pitch channel command and disturbance response and the yaw channel bandwidth. The roll channel response was judged to be satisfactory without improvement.

Fig. 10   Roll closed-loop response comparison, p/δ_{lat}.

closed-loop complex poles to verify that the system is well damped. The crossover frequency and the actuator root mean squared specifications were included for use in the control system optimization (discussed later) and drive the design to achieve the specifications with minimum overdesign. Finally, the frequency-domain pitch/roll coupling specification was included as check-only to track the influence of the feedback system on response cross coupling, but not included as an active specification in the optimization process. When the three control axes are considered, a total of 12 specifications were used in the baseline analysis.

An evaluation was first conducted on the MCLAWS-2 baseline configuration, which was the initial gain set based on linear analysis and extensive nonlinear piloted simulation. The evaluation results are shown in Fig. 11 in the form of the CONDUIT handling-quality (HQ) window. The dark gray region in each specification represents level-3 HQ ("deficiencies require improvement"), the light gray region represents level 2 ("deficiencies warrant improvement"), and the white region represents level 1 ("satisfactory without improvement"). The levels refer to the Handling-Qualities Rating scale.[1]
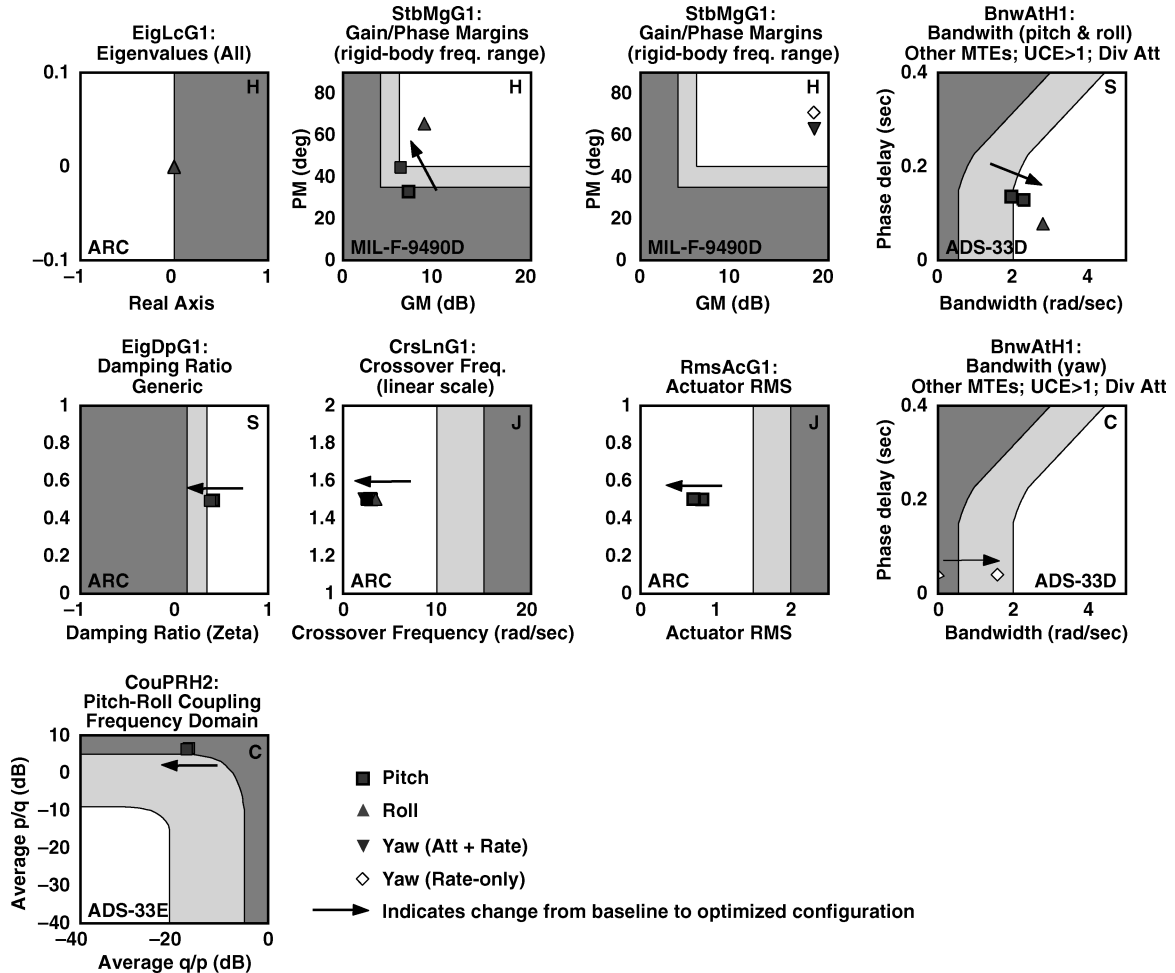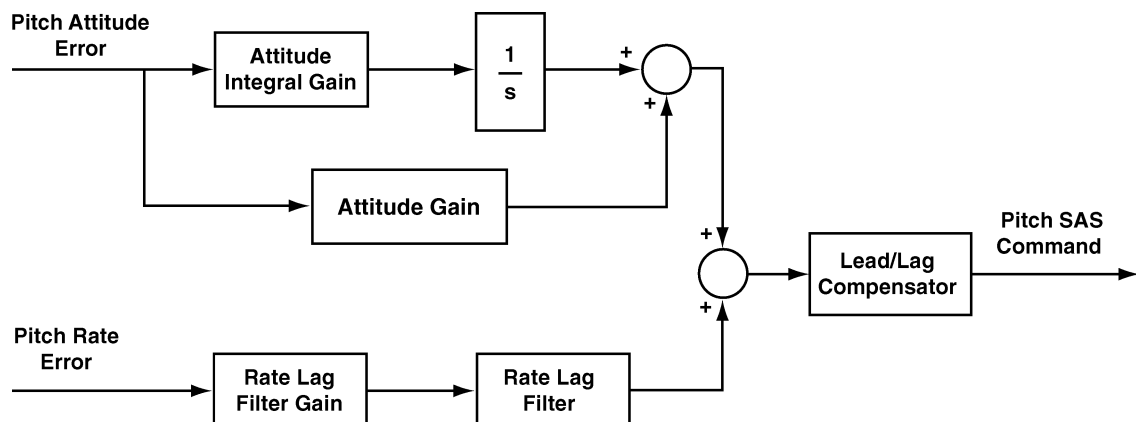
CONDUIT Optimization

The yaw bandwidth deficiency was easily resolved using CONDUIT in a manual mode. The command model frequency was increased from 2.0 to 3.3 rad/s, which brought the response to near level-1 compliance. Furthermore, increases in command model frequency resulted in excessive SAS actuator limiting. The remaining efforts in control law optimization focused on addressing the pitch axis deficiencies only. The same specifications used in the baseline evaluation were used for this optimization study.

For control law optimization in CONDUIT, the user declares each of the specifications to belong to one of the following five classes: hard constraint, soft constraint, performance objective criterion, summed objectives, or check-only.[17] The selection of specification class defines the solution strategy for the optimization process. For the pitch design optimization, the choice of constraint type for each spec is listed in Table 3. In the pitch axis MCLAWS-2 block diagram, six gains were defined as design parameters to be tuned in CONDUIT. These gains are listed in Table 4 and illustrated based on a simplified schematic of the pitch feedback loop as shown in Fig. 12.

Table 4 Relative comparison of final pitch gain sets for four configurations

Pitch SAS feedback gains	Baseline	Optimized baseline, 0% DM	8% DM	10% DM
Attitude integral gain	1.00	1.71	1.59	1.81
Attitude gain	1.00	0.58	0.47	0.38
Rate lag filter time constant	1.00	1.00	1.11	1.03
Lead/lag compensator lag time constant	1.00	0.97	0.94	0.81
Lead/lag compensator lead time constant	1.00	1.09	1.30	1.20
Rate lag filter gain	1.00	1.00	1.05	1.12

Fig. 11 CONDUIT HQ evaluation for the baseline and optimized baseline (DM = 0%) configurations.

Fig. 12 Simplified schematic of pitch feedback loop.

Optimization is conducted in three distinct phases. In phase 1, the design parameters are tuned to ensure that the hard constraints are satisfied. Selecting the stability specifications (Table 3) as hard constraints ensures that the response characteristics at the completion of phase 1 are well behaved, that is, stable, so that the remaining specifications associated with the aircraft HQ metrics will have defined values. Once all of the hard constraints meet the level-1 criteria, the optimization process moves into phase 2 and begins to work on the soft constraints while continuing to enforce compliance with the hard constraints. When the design satisfies all of the level-1 requirements for the soft and hard constraints, a feasible (but not optimal) design solution is reached, and the optimization process enters phase 3. In phase 3, CONDUIT will tune the design parameters to optimize the system based on the selected performance criteria while ensuring that the level-1 requirements are still met. In the MCLAWS-2 optimization study, the pitch crossover frequency and the actuator rms specifications were included as a summed objective function to minimize the actuator demands for piloted and turbulence inputs. This strategy ensures minimum overdesign relative to the level-1 boundaries and most important achieves the desired HQ with minimum saturation of the SAS actuators. Further detailed discussion on the CONDUIT optimization process may be found in Ref. 17.

Optimized Baseline

The optimized baseline feedback gains listed in Table 4 [indicated as 0% design margin (DM), which is explained later in this section] is the gain set obtained by CONDUIT that will just meet the minimum level-1 requirements for the specifications of Table 3. Significant changes relative to the baseline (60–70%) are seen in the integral and attitude gains that are needed to meet the level-1 requirements. Also, a lead–lag compensation with two tunable time constants was introduced to provide the added phase lead needed to achieve the required stability margins. The remaining gains are modified to less than 10%. The HQ prediction of the optimized system is shown in Fig. 11 for comparison with the baseline system. The arrow in each part shows the direction of change from the baseline to the optimized system. As can be seen, all pitch characteristics now meet the level-1 requirements. The yaw response bandwidth is now nearly level-1 as discussed earlier, and the roll response is unchanged from the baseline. These results showed the need for significant modifications to the control system configuration and gain set as obtained from the piloted simulation. This has been a common theme in the development of advanced control systems for rotorcraft.[18,19] Direct control system optimization in CONDUIT using a validated mathematical model and relevant design requirements assured that flight evaluation could proceed with a minimum of costly flight-test tuning as compared to historical experience, for example, Ref. 4.

The specifications, such as ADS-33 and MIL-F-9490D, that form the key design requirements for CONDUIT provide for the minimum response characteristics to just achieve level 1 (satisfactory without improvement). As the response is driven more deeply into the level-1 region, faster response, better disturbance rejection, and improved margin for uncertainties are all achieved, providing for improved HQ. The cost for this is increased actuator usage (which results in increased saturation) and reduced stability margins. At some point, further increases into the level-1 region cannot be achieved without 1) degradation of stability/damping into the level-2 region or 2) excessive actuator usage/saturation.

Design Margin Optimization

A DM is defined in CONDUIT as the fractional increase in the desired level-1 boundary relative to the actual specification criteria. As shown in Fig. 13, the DM is defined in terms of a fraction of the width between the level-1 and level-2 boundaries. In this example, a 10% DM sets the acceptable level-1 design boundary to a position that is inside the actual ADS-33 level 1 by a distance that is 10% of the width of the level-2 region. Thus, the nominal design to just meet ADS-33 is associated with DM = 0%. The DM optimization feature in CONDUIT automatically retunes the control system for an increasing value of DM applied uniformly to all design specifications. This results in a family of optimized solutions
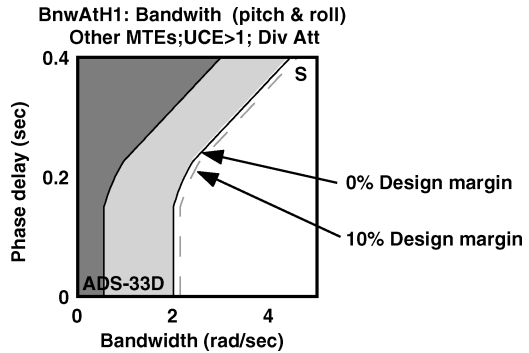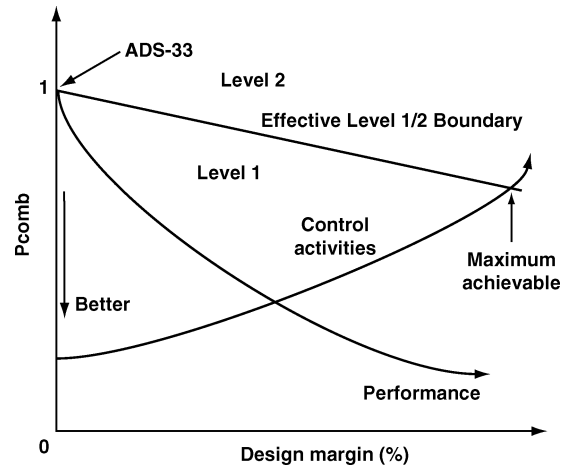

Fig. 13   Example of DM.

Fig. 14   Concept of DM optimization.

based on uniformly increasing performance into the level-1 region. As the design margin is increased, the optimization engine attempts to drive all of the constraint specifications further into the level-1 region, until one or more specifications fails to achieve the more stringent criteria. The final candidate designs are selected by the users from user's assessment of the tradeoff between performance improvement and actuator usage as embodied in the family of solutions obtained by CONDUIT. This greatly reduces the number of configurations ultimately to be flight tested as compared to the traditional approach, for example, Ref. 4.

Figure 14 shows the typical tradeoff behavior for a range of design margin values. Note that units for the y axis of Fig. 14 are in terms of the performance comb (Pcomb). As discussed in more detail in Ref. 20, the Pcomb is a normalized value of the numerical rating of the design point on each specification in CONDUIT. A value of Pcomb = 1 indicates that the design point lies on the level-1 boundary, and a value Pcomb < 1 indicates how far the design point is into the level-1 region. Thus, a lower value of Pcomb indicates improved performance. As mentioned in the example earlier, a 10% DM sets the level-1/level-2 boundary 10% of the width of the level-2 region into the level-1 region of a specification. The new boundary is now the effective level-1/level-2 boundary of the specification. Thus, a Pcomb value of 0.9 now indicates that the design point lies on the level-1/level-2 boundary for the 10% DM case.

As shown in Fig. 14, a control system is initially designed and optimized to just meet ADS-33 with 0% DM. As the DM increases, which implies that the level-1 region of all of the specifications is smaller, better overall performance (faster response, improved agility, better stability, for instance) can be achieved at the expense of increased control activity (leading to saturation) and degraded stability margins. Eventually, as shown in Fig. 14, the control activity (and stability) specifications intersect the effective level-1/level-2 boundary, and no further increase in DM is possible. The MCLAWS-2 design was optimized for increasing values of DM using the CONDUIT DM optimization feature. Figures 15a–15e show
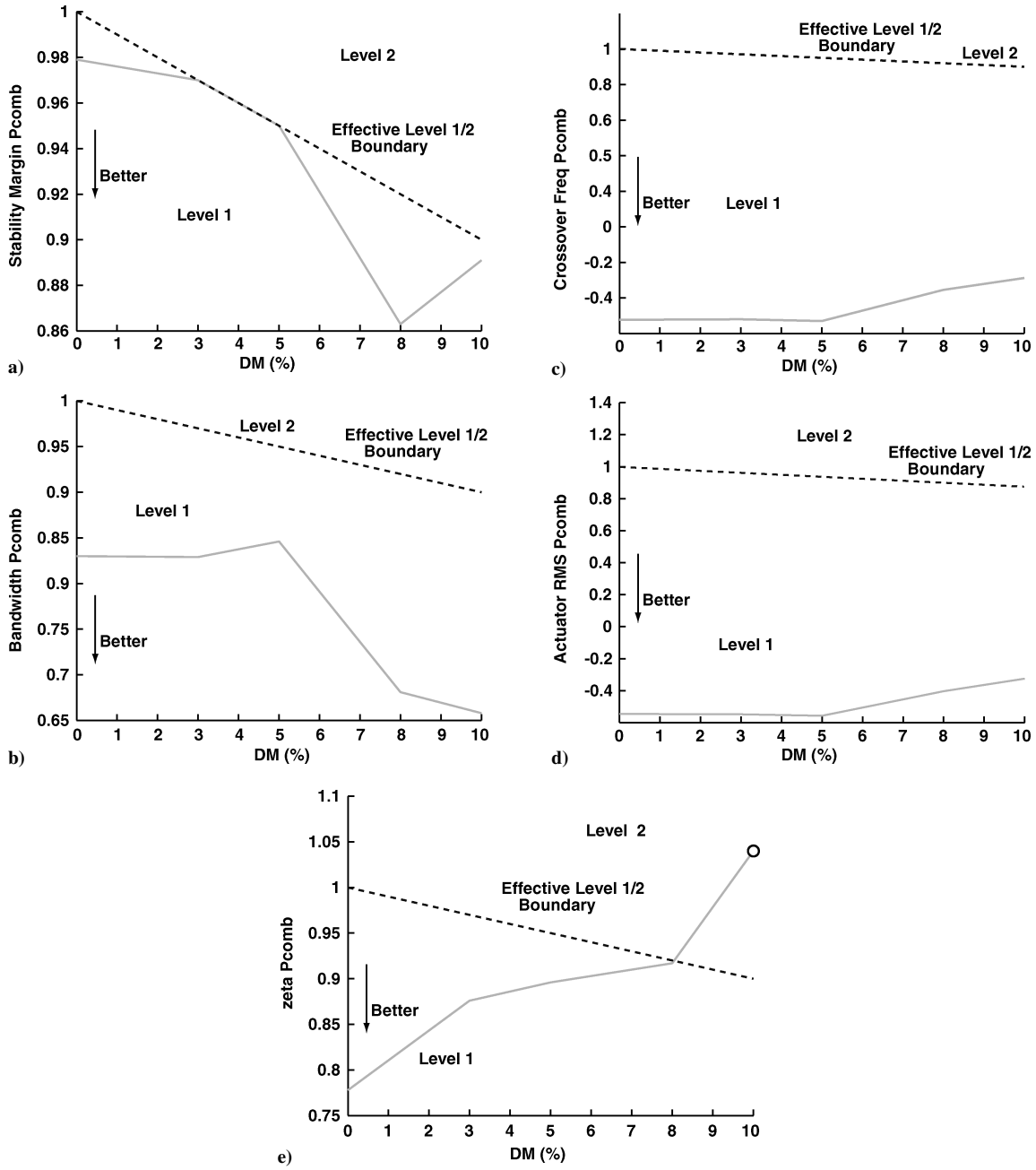
Fig. 15 DM optimization: a) stability margin, b) bandwidth, c) crossover frequency, d) actuator rms, and e) damping ratio.

the effect of increasing DM on the various pitch specifications, in terms of the Pcomb values.

As the DM is increased, both the pitch stability margin (Fig. 15a) and bandwidth (Fig. 15b) specifications are driven further into level-1, which implies better stability and responsiveness. The increase in bandwidth is achieved by an increase in the crossover frequency, as can be seen in Fig. 15c. The increased bandwidth also increases frequency and amplitude of the pitch actuator demands as expected (Fig. 15d). Eventually the drive for increased crossover frequency causes the pitch stability margin and closed-loop damping ratio to be reduced to where they cross over the level-1 boundary and enter the level-2 region. The pitch damping ratio now cannot achieve level-1 performance for the 10% DM (circle symbol in Fig. 15e). Further increases in DM are not achievable, and so the optimization stops at this point. Recall that originally, the damping ratio performance was solidly in the level-1 region for the DM = 0% design. Such behavior confirmed the expected tradeoff trends discussed earlier.

Figure 16 shows the overlay of HQ windows for DM = 0, 8, and 10%. The effect of increasing DM is indicated by the gray arrows

and reflects the performance trends of Fig. 15a–15e. Table 4 shows the comparison of the gain sets of these three configurations relative to the normalized baseline set.

From this study, it can be concluded that the 8% DM case is the optimum case, with all of the specifications meeting level-1 criteria and significant improvements in HQ and performance, while maintaining reasonable demands on actuator activity. The 10% DM case yields improvement in the design responsiveness, but with a less well-damped response to disturbances. As discussed later, flight tests were conducted to evaluate the HQ tradeoff between the 8 and 10% DM design, and the pilots' consensus was preference for the 10% DM case, which provided increased responsiveness albeit with slightly reduced damping. The 10% DM design was evaluated for robustness to uncertainties in the identified mathematical model parameters, as discussed next.

Robustness Analysis for 10% DM Case

The robustness of the 10% DM design was examined by using the Robustness Analysis Tool in CONDUIT. This tool analyzes the
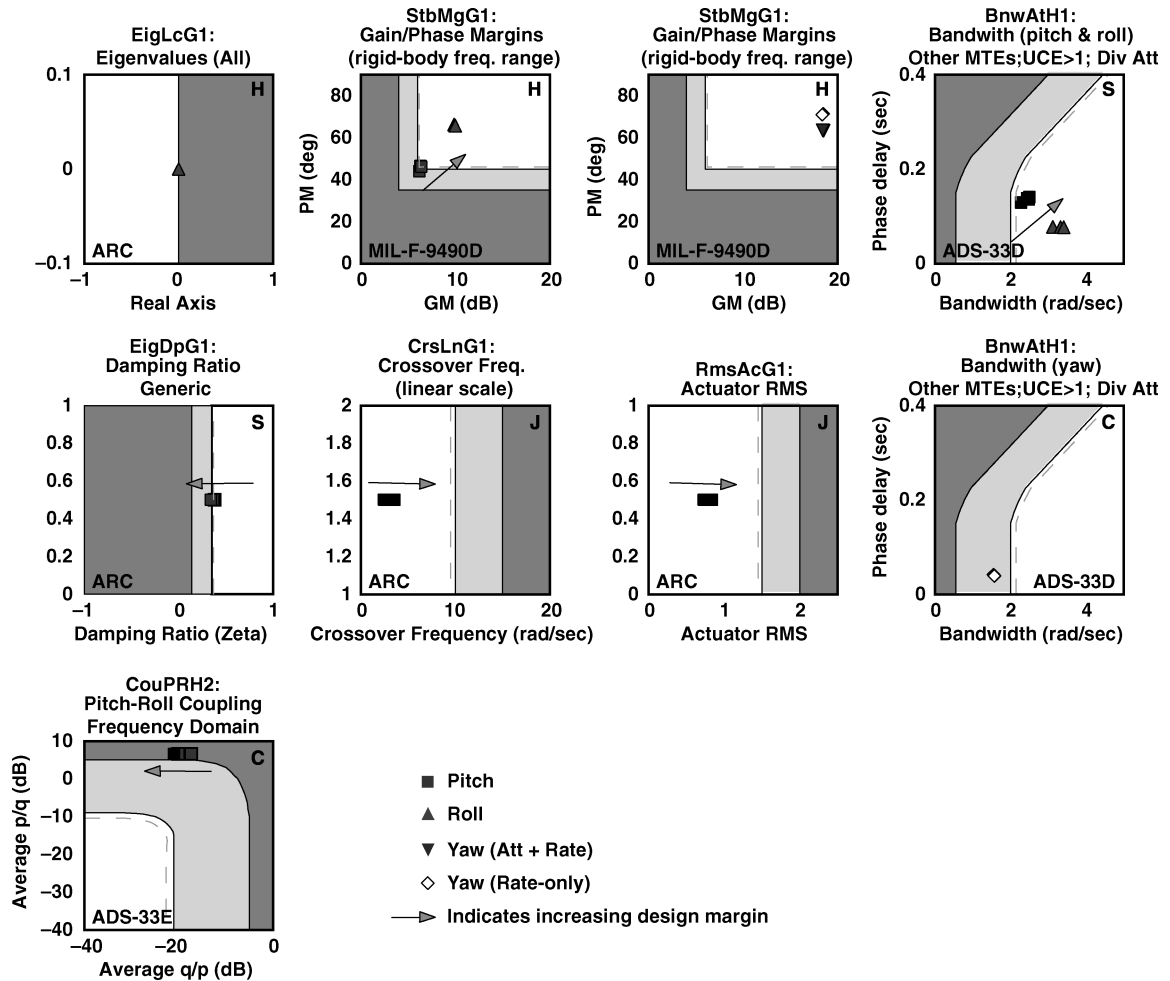
EigLcG1: Eigenvalues (All)

StbMgG1: Gain/Phase Margins (rigid-body freq. range)

StbMgG1: Gain/Phase Margins (rigid-body freq. range)

BnwAtH1: Bandwith (pitch & roll) Other MTEs;UCE>1; Div Att

EigDpG1: Damping Ratio Generic

CrsLnG1: Crossover Freq. (linear scale)

RmsAcG1: Actuator RMS

BnwAtH1: Bandwith (yaw) Other MTEs;UCE>1; Div Att

CouPRH2: Pitch-Roll Coupling Frequency Domain

■ Pitch
▲ Roll
▼ Yaw (Att + Rate)
◇ Yaw (Rate-only)
→ Indicates increasing design margin

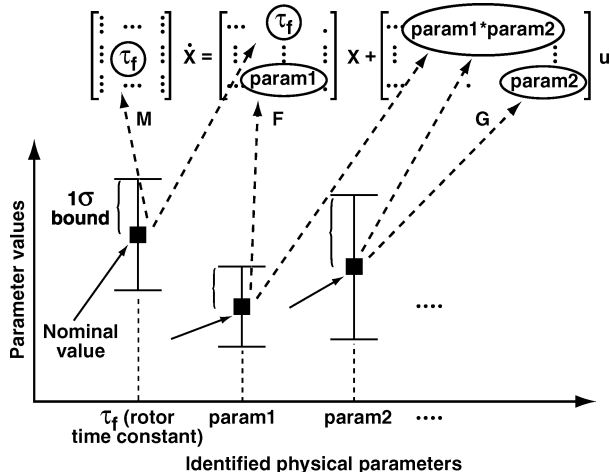**Fig. 16 HQ window overlay of DM = 0, 8, and 10%.**

Fig. 17 Example of how CIFER identified physical parameters relate to aircraft state-space model.

variation in predicted HQ and performance with respect to parametric model uncertainties.

The full state-space CIFER identified model for the UH-60 as described in Eq. (1) contains 61 identified physical parameters. These parameters have been propagated to 82 entries throughout the system matrices, M, F, and G, in Eq. (1), as shown in Fig. 17. For each identified physical parameter, CIFER provides both the nominal value and the associated statistical 1σ confidence bound as shown in Fig. 17. All of the analyses conducted in CONDUIT described thus

far were based on using the nominal values of the identified physical parameters as reflected in the matrices M, F, and G in Eq. (1). The parametric model uncertainties considered in the present robustness analysis are based on the 1σ perturbation bounds of the identified physical parameters, not on direct independent perturbations of the elements of the matrices in Eq. (1). More specifically, the parametric model uncertain control system considered in this study can be described as

$$(M + \Delta M)\dot{x} = (F + \Delta F)x + (G + \Delta G)u$$

$$y = Hx + Ju \qquad (5)$$

where M, F, G, H, and J are matrices of nominal values for the identified aircraft model and all of the parametric model uncertainties are contained in ΔM, ΔF, and ΔG matrices.

As shown in Fig. 17, it is important to note that there are identified physical parameters that appear in multiple entries in Eq. (1), such as the rotor flapping time constant τ_f, which appears in both the M and F matrices. As a result, the 1σ perturbation to τ_f, for example, $\Delta\tau_f$, would also appear in both ΔM and ΔF matrices in Eq. (5). Moreover, as shown in Fig. 17, some entries in Eq. (1) could be constrained by one or multiple identified physical parameters; such as *param1* in the F matrix, and *param2* and *param1 ∗ param2* in the G matrix. In this case, the 1σ perturbations to *param1* and *param2*, for example, $\Delta param1$ and $\Delta param2$, would propagate accordingly to the ΔF and ΔG matrices. Therefore, for example, the perturbation term corresponding to *param1 ∗ param2* in the ΔG matrix is (*param1 ∗ Δparam2 + param2 ∗ Δparam1 + Δparam1 ∗ Δparam2*).

The characterization of uncertainty for the state-space model is, thus, seen to be highly structured owing to the relationships between
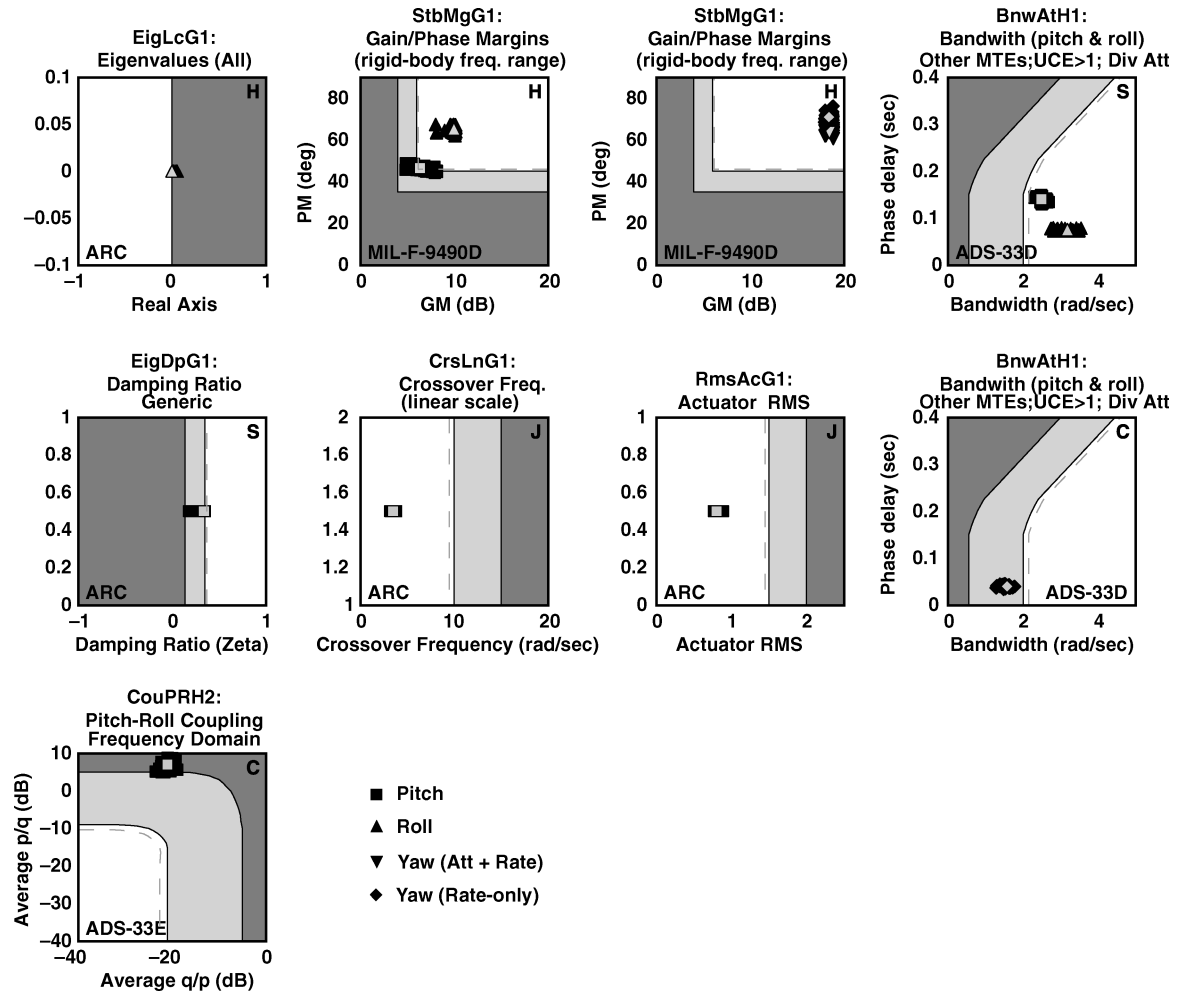
Fig. 18 Robustness analysis of DM = 10%; light color symbol, nominal case.

the identified physical parameters and the state-space model matrices. These same relationships define the structure of the uncertainties in the state-space matrices. Hence, the class of uncertain systems described in Eq. (5) is quite different from that commonly considered in the context of robust/H^∞ control design methods (e.g., Ref. 21), where the uncertainty is assumed to be unstructured and belong to some norm-bounded set. Furthermore, when the leading term $M + \Delta M$, which is invertible for all admissible ΔM, is inverted and multiplied through Eq. (5) to form the standard state-space representation, the resultant uncertain system description would be more complex (and the robustness of its control system more difficult) to analyze by using the robust/H^∞ control approaches. The CONDUIT Robustness Analysis Tool, on the other hand, was developed to handle the uncertain control systems with the actual structured parametric model uncertainties as described in Eq. (5). Tischler et al.[22] compare the robustness of several popular control design methods (classical feedback, model following, LQR, and H^∞) by using this same capability. In the discussion that follows, we present the detailed robustness analysis procedure and results for the 10% DM design solution.

The CONDUIT/CIFER integration routines that are part of CONDUIT allow direct extraction of the CIFER identified aircraft model and associated 1σ perturbation bounds from the CIFER database. A randomized set of cases are formed by first perturbing the actual identified parameters and propagating them throughout, ΔM, ΔF, and ΔG, in Eq. (5). Each perturbed case is then converted to standard state-space form:

$$\dot{x} = Ax + Bu, \qquad y = Cx + Du \qquad (6)$$

for evaluation in CONDUIT. A total of 30 perturbation cases were simulated in CONDUIT. The perturbation increment for a particular

identified parameter is randomly selected as the $+1\sigma$ or -1σ value of the uncertainty bound for the parameter as given in Ref. 9. A single perturbation case is formed by simultaneously varying all of the identified physical parameters with the randomized value ($+1\sigma$ or -1σ) as appropriate to each parameter and then conducting the HQ analysis.

The evaluation of the 30 perturbed cases is shown along with the nominal case, that is, no perturbation, in Fig. 18. The nominal case is highlighted (light color), whereas all other perturbed cases shown in the dark colored symbols. It can be seen in Fig. 18 that the performance of all of the perturbed cases remain fairly close to that of the nominal case. In most cases, the specification values remain in either the level 1 or level 2 region. The key exception is the eigenvalue specification (EigLcG1), which crosses into the level 3 region, indicating instability for some perturbed cases. However, examination of these perturbed cases reveals that the instability was caused by some very low-frequency unstable poles in the closed-loop system. (The fastest pole is at 0.05 rad/s.) These very low-frequency modes have time constants that are slow enough, that is, greater than 20 s to be inconsequential for the perturbed cases, and no evidence of long-term instability was apparent in the flight tests. Overall, it can be concluded that the 10% DM MCLAWS-2 configuration can be expected to be robust to uncertainties in the aerodynamic parameters.

Flight Test Evaluation of Optimization Cases

Following CONDUIT optimization, quick piloted assessments were obtained using the RIPTIDE real-time simulation capability. The assessment provided the safety pilot with an important initial impression and a high degree of confidence before RFCC
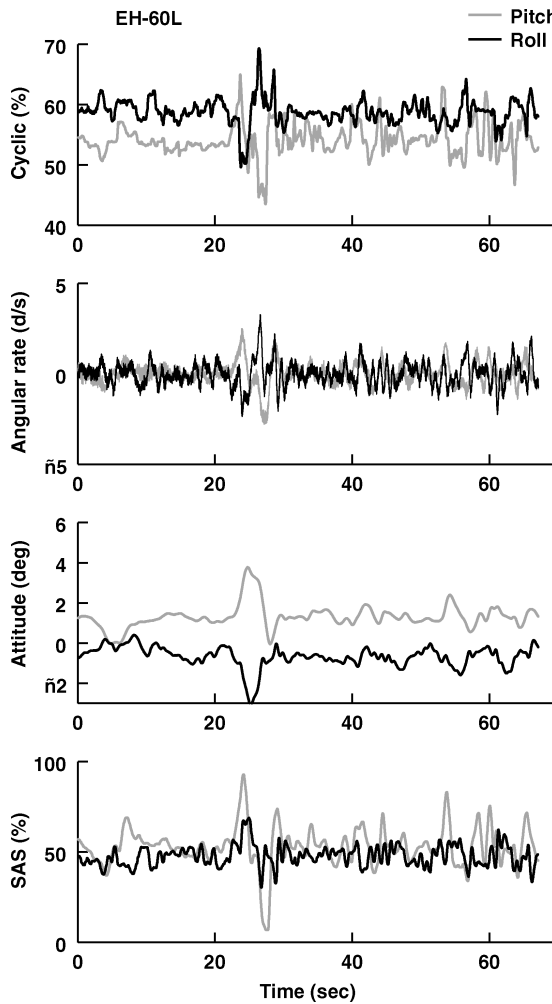
Fig. 19   Time history of EH-60L BLACK HAWK SAS/FPS standard control laws for the ADS-33 hover maneuver.

engagement. Flight assessments of the various MCLAWS-2 configurations were performed on the U.S. Army/NASA EH-60L aircraft. These flight evaluations focused on the comparison of the standard EH-60L SAS/FPS vs the optimized configurations (0, 8, and 10% DM cases). Initial assessments were made from control pulse inputs in each axis, but it was difficult to select an overall best configuration based on the single-axis inputs. To assess these configurations in a more multi-axis control task, the ADS-33 hover maneuver was performed. The maneuver cueing and performance standards were the same as developed and used for Ref. 23.

Figure 19 shows a sample time history for the EH-60L with the standard SAS/FPS performing the ADS-33 hover maneuver. Figure 20 shows the same hover maneuver for the various optimized configurations (0, 8, and 10% DM), respectively. As the DM increases from 0 to 10%, there is a noticeable reduction in piloted stick activity, increased crispness in response to control inputs, and improved disturbance rejection during periods of no piloted inputs. Note that with the 10% DM case, hands-off performance was possible in low-wind conditions for durations of 3–4 s following the deceleration. Notice also that except for the 1–2 s of longitudinal saturation just after the 20-s point in the time history (Fig. 20, 10% DM), there is almost no evidence of actuator saturation for the MCLAWS-2 partial authority system implementation.

Pilot comments from the hover maneuver with the 10% DM case show that the pilots were able to make a smooth deceleration into the hover position and that maintaining a stabilized hover required a low pilot workload (minimal pilot input required). Pilot comments from the 8% DM case indicate that the aircraft open-loop response was very stable in all axes, but the aircraft was somewhat difficult to stabilize with the pilot in the loop. For the baseline configuration, the pilots commented that more workload was required to maintain desired performance standards due to lateral and longitudinal drift. In the end, a consensus was reached that the 10% DM configuration indeed yielded the best overall performance.

To assess the 10% DM configuration in a broader evaluation, the 10% DM configuration and the EH-60L standard SAS/FPS configuration were evaluated while performing the ADS-33 hover, vertical, lateral reposition, and departure/abort maneuvers. In addition, an SAC-developed maneuver, called an aggressive approach to hover, was also evaluated.
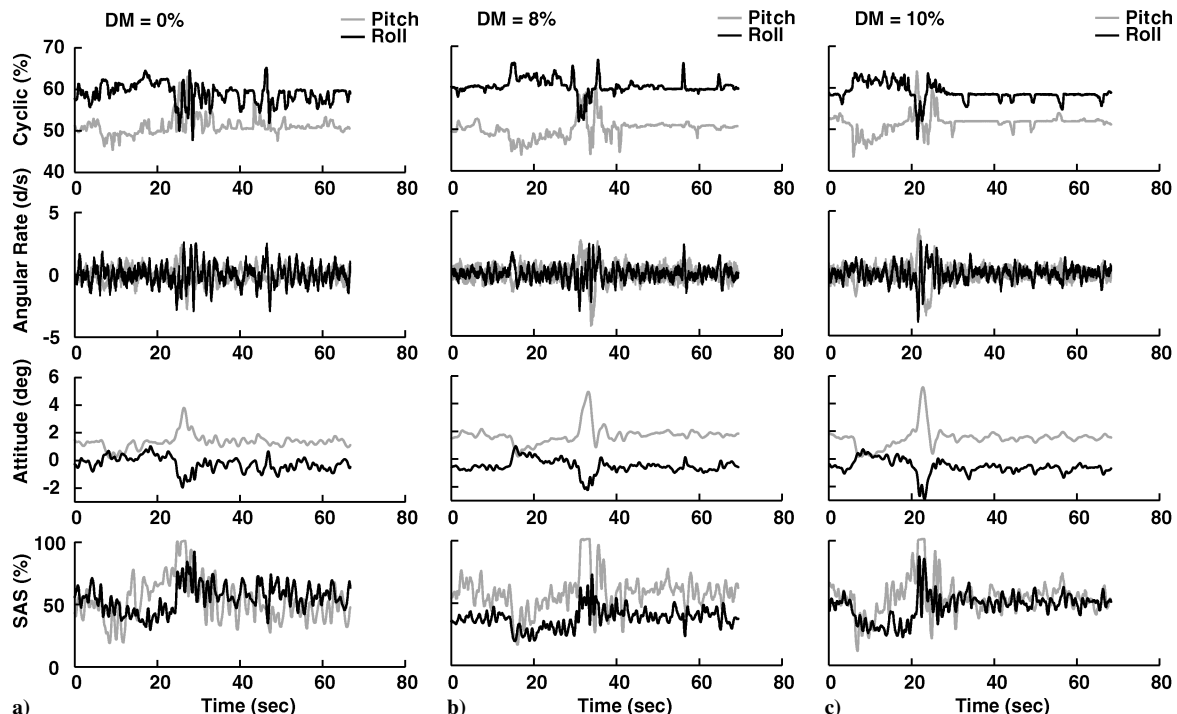

Fig. 20   Comparison of MCLAWS-2 optimized for varying DMs for ADS-33 hover maneuver: a) 0% DM, b) 8% DM, and c) 10% DM.
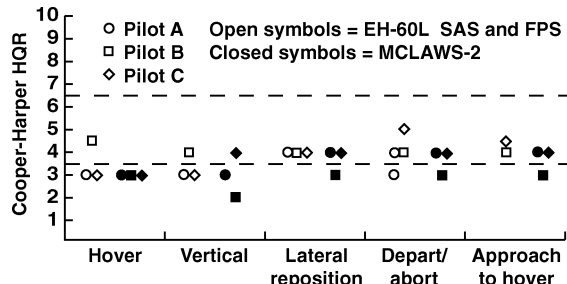
Fig. 21 HQ evaluations of MCLAWS-2 and EH-60L standard SAS/FPS.

The following are typical comments for hovering flight for the standard EH-60L: 1) "At the edge of 'desired' performance—going into 'adequate' performance," 2) "No unacceptable oscillations, but some oscillations," 3) "Same strategy as with MCLAWS, but a lot more control inputs required with baseline BLACK HAWK," 4) "Off-axis coupling higher than with MCLAWS," and 5) "Cooper–Harper handling qualities rating (HQR) = 4."

The following are typical comments for hovering flight with the MCLAWS (10% DM) system: 1) "Not that difficult to get into 'desired' performance," 2) "Easy to predict aircraft response," 3) "No differences observed in inceptor forces between baseline BLACK HAWK and MCLAWS," 4) "No harmony problems," 5) "No oscillations," 6) "Feet off the pedals—heading hold keeps response within 'desired' performance," 7) "No compensation required for any aircraft deficiencies," and 8) "Cooper–Harper handling qualities rating (HQR) = 2."

Figure 21 shows the Cooper–Harper HQ ratings[24] for the five maneuvers from three pilots. The results show a consistent but small improvement with MCLAWS-2 compared to the EH-60L standard SAS/FPS configuration. The sample time histories (Fig. 19 vs Fig. 20, 10% DM), pilot evaluations (Fig. 21), and associated comments (just summarized) indicate that compared to the EH-60L standard SAS/FPS configuration the 10% DM MCLAWS-2 configuration has less control activity, is more predictable, requires less pilot workload, and overall shows significant benefits. It should be remembered that this comparison was conducted on a calm, clear day, and the primary advantage or benefit of the attitude command control laws is realized in the degraded visual environment. Suggestions raised early in the project that the added stability of an attitude command response type might appear sluggish to the pilot in the day (good visual environment) did not prove to be a concern in flight.

The utility of the MCLAWS-2 system is limited to hover and near-hover (20–30 kn), beyond which significant saturation of the 10% authority occurs due to the trim demands. Incorporating a parallel trim outer loop (in the MCLAWS-1 integrated configuration) offloads the trim requirement as discussed in Ref. 2. These MCLAWS-1 flight-test results show that the short-term HQ and stability improvements achieved herein using the 10% authority series implementation can be extended to 50 kn.

Conclusions

An initial set of MCLAWS-2 was developed for and evaluated on an EH-60L helicopter in a rapidly executed program. Central to addressing the significant resource and technical challenges of this project was the extensive use of a modern integrated tool set, comprised of block diagram simulation (SIMULINK), system identification (CIFER), control system analysis and optimization (CONDUIT), real-time rapid prototyping (RIPTIDE), and pictures-to-code conversion.

The key findings were as follows:

1) A short, focused program of ground test and frequency-sweep flight tests (1 h of flight data) of the MCLAWS-2 baseline gain set allowed the comprehensive validation and updating of the mathematical model to be completed using system identification methods. This provided a validated anchor point as the basis for reliable control system optimization.

2) Control system optimization to meet the desired HQ criteria for the validated analysis model resulted in significant modifications to the baseline configuration as obtained from the piloted simulation.

3) A family of optimized designs was determined for increasing values of DM, thus achieving a uniform increase in predicted performance relative to the ADS-33 minimum requirements. The optimized design (with 10% DM) was shown to be robust to uncertainty in the identified physical parameters.

4) A flight-test evaluation by three test pilots showed significant benefits of the MCLAWS-2 attitude-response-type system with an optimized gain set (10% DM) compared to the EH-60L standard SAS/FPS system. For the modernized system, there was a noticeable reduction in piloted stick activity, increased crispness in response to control inputs, and improved disturbance rejection during periods of no piloted inputs.

References

[1]"Aeronautical Design Standard, Handling Qualities Requirements for Military Rotorcraft," U.S. Army Aviation and Missile Command, USAAM-COM Rept. ADS-33E-PRF, March 2000.

[2]Sahasrabudhe, V., Blanken, C. L., Faynberg, A., and Hindson, W., "Modernized Control Laws: From Design to Flight Test," American Helicopter Society 4th Decennial Specialist's Conf. on Aeromechanics, Jan. 2004.

[3]Sahasrabudhe, V., Blanken, C. L., Melkers, E., and Faynberg, A., "Piloted Evaluation of Modernized Limited Authority Control Laws in the NASA-Ames Vertical Motion Simulator (VMS)," American Helicopter Society 59th Annual Forum Proceedings, May 2003.

[4]Robinson, D., Brunson, K., Davis, A., Klase, S., Garrett, E., and Kelly, C., "OH-58D(R) Stability and Control Augmentation System Optimization," Development Test Command, DTC Project 4-AI-130-58D-077/KF, Fort Rucker, AL, Nov. 2003.

[5]"Using Simulink®," MathWorks, Inc., Natick, MA, Nov. 2000.

[6]Tischler, M. B., and Cauffman, M. G., "Frequency-Response Method for Rotorcraft System Identification: Flight Applications to BO-105 Coupled Rotor/Fuselage Dynamics," *Journal of the American Helicopter Society*, Vol. 37, No. 3, 1992, pp. 3–17.

[7]"CONDUIT® Version 4.1 User's Guide," Raytheon, Rept. ITSS 41-071403, Moffett Field, CA, July 2003.

[8]Mansur, M., Frye, M., and Montegut, M., "Rapid Prototyping and Evaluation of Control Systems Designs for Manned and Unmanned Applications," American Helicopter Society 56th Annual Forum Proceedings, May 2000.

[9]Fletcher, J. W., and Tischler, M. B., "Improving Helicopter Flight Mechanics Models with Laser Measurements of Flapping," American Helicopter Society 53rd Annual Forum Proceedings, April–May 1997.

[10]"Real-Time Workshop User's Guide," MathWorks, Inc., Natick, MA, Nov. 2000.

[11]Howlett, J. J., "UH-60A Black Hawk Engineering Simulation Program: Volume I—Mathematical Model," NASA CR-166309, Dec. 1981.

[12]Tischler, M. B., "System Identification Requirements for High-Bandwidth Rotorcraft Flight Control System Design," *Journal of Guidance, Control, and Dynamics*, Vol. 13, No. 5, 1990, pp. 835–841.

[13]Frost, C. R., Hindson, W. S., Moralez, E., Tucker, G., and Dryfoos, J. B., "Design and Testing of Flight Control Laws on the RASCAL Research Helicopter," AIAA Paper 2002-4869, Aug. 2002.

[14]Lusardi, J., Blanken, C., and Tischler, M. B., "Piloted Evaluation of a UH-60 Mixer Equivalent Turbulence Simulation Model," American Helicopter Society 59th Annual Forum Proceedings, May 2003.

[15]Sahasrabudhe, V., Spaulding, R., Faynberg, A., Horn, J., and Sahani, N., "Simulation Investigation of a Comprehensive Collective-Axis Tactile Cueing System," American Helicopter Society 58th Annual Forum Proceedings, June 2002.

[16]Williams, J. N., Ham, J. A., and Tischler, M. B., "Flight Test Manual: Rotorcraft Frequency Domain Flight Testing," U.S. Army Aviation Technical Test Center, Airworthiness Qualification Test Directorate, AQTD Project 93-14, Edwards AFB, CA, Sept. 1995.

[17]Tischler, M. B., Colbourne, J., Morel, M., Biezad, D., Cheung, K., Levine, W., and Moldoveanu, V., "A Multidisciplinary Flight Control Development Environment and Its Application to a Helicopter," *IEEE Control Systems Magazine*, Vol. 19, No. 4, 1999, pp. 22–33.

[18]Tischler, M. B., Fletcher, J. W., Morris, P. M., and Tucker, G. E., "Flying Quality Analysis and Flight Evaluation of a Highly Augmented Combat Rotorcraft," *Journal of Guidance, Control, and Dynamics*, Vol. 14, No. 5, 1991, pp. 954–964.

[19]Crawford, C. C., "Potential for Enhancing the Rotorcraft Development/ Qualification Process Using System Identification," NATO Research and Technology Organization Systems Concepts and Integration Symposium on System Identification for Integrated Aircraft Development and Flight Testing, RTO-MP-11, May 1998.

[20]Colbourne, J. D., Frost, C. R., Tischler, M. B., Cheung, K. K., Hiranaka, D. K., and Biezad, D. J., "Control Law Design and Optimization for Rotorcraft Handling Qualities Criteria Using CONDUIT," American Helicopter Society 55th Annual Forum Proceedings, May 1999.

[21]Skogestad, S., and Postlethwaite, I., *Multivariable Feedback Control: Analysis and Design*, Wiley, New York, 1996, pp. 384–388.

[22]Tischler, M. B., Lee, J. A., and Colbourne, J. D. "Comparison of Alternative Flight Control System Design Methods Using the CONDUIT® Design Tool," *Journal of Guidance, Control, and Dynamics*, Vol. 25, No. 3, 2002, pp. 482–493.

[23]Blanken, C. L., Cicolani, L., Sullivan, C. C., and Arterburn, D. R., "Evaluation of Aeronautical Design Standard-33 Using a UH-60A Black Hawk," American Helicopter Society 56th Annual Forum Proceedings, May 2000.

[24]Cooper, G. E., and Harper, R. P., "The Use of Pilot Rating in the Evaluation of Aircraft Handling Qualities," NASA TN D-5153, April 1969.